



# Optical and electronic correlation in Mg-doped nano cadmium sulfide

Zein K. Heiba<sup>1</sup> · Mohamed Bakr Mohamed<sup>1,2</sup> · Sameh. I. Ahmed<sup>3</sup>

Received: 26 October 2020 / Accepted: 17 April 2021 / Published online: 2 May 2021  
© The Author(s), under exclusive licence to Springer Science+Business Media, LLC, part of Springer Nature 2021

## Abstract

Nano  $\text{Cd}_{0.9}\text{Mg}_{0.05}\text{S}$  was synthesized applying the thermolysis technique in air and under flow of nitrogen. Samples obtained exhibited CdS structure with two phases. Rietveld refinement analysis was used to determine the different structure parameters. Analysis of UV–Vis absorption spectra disclosed that the optical band gap of CdS sample prepared in  $\text{N}_2$  is less than that of the corresponding sample prepared in air. The optical band gap of CdS (air) sample was decreased as it doped with Mg while it increased as Mg doped CdS ( $\text{N}_2$ ) sample. The photoluminescence (PL) intensities of CdS samples were enhanced when they doped with Mg. Moreover, the PL intensity of CdS (air) increased further as it prepared under nitrogen. The emitted PL colors (violet, blue and green) depended on the condition of preparation of the different samples. Density functional theory calculation (DFT) was applied to explain the variation in the optical band gap of CdS upon doping with Mg. DFT calculation revealed that the absorption, refractive index, extinction coefficient, the dielectric properties and photoconductivity response were affected by the kind of defects in the sample. Mg-doped stoichiometric or non-stoichiometric CdS have a non-magnetic nature.

**Keywords** Mg-doped CdS · Size · Optical · Electronic

## 1 Introduction

Semiconductor materials such as CdS, CdSe and CdTe are widely applied in many applications due to their optical characteristics (Yellaiah et al. 2014). CdS is member of II–VI chalcogenide materials that have a direct band gap of 2.42 eV and a small exciton Bohr

---

✉ Mohamed Bakr Mohamed  
mbm1977@yahoo.com

✉ Sameh. I. Ahmed  
a.sameh@tu.edu.sa

<sup>1</sup> Physics Department, Faculty of Science, Ain Shams University, Cairo 11566, Egypt

<sup>2</sup> Physics Department, Faculty of Science, Taibah University, Al-Madina al Munawarah 42353, Saudi Arabia

<sup>3</sup> Department of Physics, College of Science, Taif University, P.O. Box 11099, Taif 21944, Saudi Arabia

radius of 3 nm (Giribabu et al. 1512). Nano CdS has excellent optical behaviors such as visible-light yield and appropriate conduction band potential for the photocatalytic applications (Pan et al. 2012). Furthermore, it can use in several applications such as solar cells, LED, flat panel displays, luminescent devices, labeling, imaging and sensor applications (Murphy 2002; Sakthivel et al. 2018). CdS can be formed in one or more phases (zinc blende or wurtzite or rock-salt) (Heiba et al. 2015a). The hexagonal and rock salt phases can be produced with ambient and high pressure conditions, respectively (Mueller et al. 2005). As the crystallite size of CdS reduced, a cubic structure can be obtained (Mueller et al. 2005). The phase transformation of CdS from one phase to another depends on many aspects for instance vacancies and interstitial of cadmium and stacking faults imperfections (Morales et al. 2001). As the crystallite size of CdS lies between 4–5 nm, CdS with both cubic and hexagonal phases can be obtained, only one phase can be found as the crystallite size of CdS is less or larger than 4–5 nm (Banerjee et al. 2000). First principle study revealed that  $(\text{CdS})_n$  ( $n = 1-8$ ) cluster exhibited nonlinear optical responses due to the production of absorption peaks in the UV and visible ranges (Pegu et al. 2018). Also the thermodynamics characteristics of the  $(\text{CdS})_n$  cluster were increased as the temperature and the size of the cluster increased (Pegu et al. 2018). Density functional calculations showed that planar CdS sheet can be used in visible light photo-catalysis due to its lower band gap (Garg et al. 2016). In the photocatalyst applications of CdS, the production of recombination sites between photogenerated electrons is expected (Li et al. 2011, 2008). To solve this problem, suitable impurities can introduce inside CdS material, which can modulate its physical and chemical characteristics (Yücel and Beleli 2018). First principle study showed that the adaptable conducting character of the V or Cr-doped CdS monolayer nominated them to be used as a spin filter, create metal–semiconductor interface etc.... (Deb et al. 1953). On the other hand, the optical band gap of Mg-doped materials depends on the kind of the host materials, amount of Mg-doping, the dimension of the sample (1D, 2D or 3D) and the method of preparation. Devadoss et al. demonstrated that nano  $\text{Cd}_{0.9-x}\text{Zn}_{0.1}\text{Mg}_x\text{S}$  material could choose for luminescence labels and imaging uses because its wide range of band gap, high optical transmittance and high photoluminescence emission (Devadoss and Sakthivel 2020). Yücel et al. found that the band gap of Mg-doped PbS thin film occurred within the solar spectral region (Yücel and Beleli 2018). Furthermore, Mg-doped PbS thin film (p-type semiconductor material) may be used as another buffer layer material for perovskite solar application (Yücel and Beleli 2018). The high optical transparency and low electrical resistivity values obtained in Mg-doped CdS films nominated them to be used as a potential candidate for a window material in solar cell uses (Sivaraman et al. 2014). Nanocomposite CdS/Mg–PVA has a notable improvement in the degradation of pollutants when irradiated with visible light (Krishnakumar et al. 2017). The optical energy gaps of CdS doped by 10%Mg prepared in air or underflows of nitrogen were increased in both cases as compared with undoped samples (Mohamed et al. 2018). The optical properties for nano ZnO have been changed significantly as it doped with Mg (Heiba et al. 2015b). The optical band gap of nano CdTe thin film increased (Kobyakov 2014), while it decreased in PbS or nano  $\text{Cd}_{0.9}\text{Zn}_{0.1}\text{S}$  or nano CdS samples as they doped with Mg (Giribabu et al. 1512; Yücel and Beleli 2018; Devadoss and Sakthivel 2020; Sivaraman et al. 2014). In this study, the reason for increasing or decreasing the band gap of CdS upon doping with 5%Mg is discussed using DFT calculation. The photoconductivity response of undoped and Mg-doped CdS (stoichiometric or non-stoichiometric) was also investigated. Therefore, CdS:5%Mg was prepared using the thermolysis technique in air and  $\text{N}_2$  atmospheres. The structural, microstructural, optical and electronic characteristics of the formed samples were explored in detail.

## 2 Methods and materials

CdS and  $\text{Cd}_{0.9}\text{Mg}_{0.05}\text{S}$  were synthesized using cadmium and magnesium acetates ( $\text{Cd}(\text{CH}_3\text{COO})_2 \cdot 2\text{H}_2\text{O}$ , 98% and  $\text{Mg}(\text{CH}_3\text{COO})_2 \cdot 4\text{H}_2\text{O}$ , 99%) and thiourea ( $\text{SC}(\text{NH}_2)_2$ , 99.98%) which were mixed simultaneously under two circumstances (air,  $\text{N}_2$  flow): The amount of cadmium acetate to thiourea was (1:1 and 1: 3) in both cases, respectively. The powders in both cases were mixed and then heated at 220 and 300 °C in air and under  $\text{N}_2$  flow in an electric oven, respectively (Mohamed et al. 2018). MAUD program relied on Rietveld profile procedure was applied on X-ray diffraction ((X'pert MPD, Philips, copper source) to find the crystal structure and microstructure of the different samples (Lutterotti 2010; Rodríguez-Carvajal 1993). Identification of all elements in each sample was examined by scanning electron microscope (FE-SEM, Quanta FEG-250). UV-vis and the photoluminescence spectra were performed using Shimadzu UV-3101PC UV-Vis-NIR and RF-1501 SHIMADZU, Ltd technique. Different electronic structure parameters were obtained applying Cambridge sequential total energy package (CASTEP) software (Perdew et al. 1996a) which relied on the first principle calculation. The supercell (211) of the cubic CdS phase, ultra-soft pseudopotentials and GGA-PBE condition were used during the calculation (Perdew and Wang 1992; Perdew et al. 1996b). The  $4d^{10}5s^2$ ,  $2p^63p^2$  and  $3s^23p^4$ , electrons related to Cd, Mg and S atoms were used as pseudopotential arrangements, respectively. The electronic properties of CdS and Mg-doped (CdS,  $\text{Cd}_{1-\delta}\text{S}$ ,  $\text{CdS}_{1-\delta}$  and  $\text{CdS}_{1-\delta}\text{O}_\delta$ ) samples were investigated.

The absorption coefficient,  $\alpha(\omega)$ , and the refractive index of the material ( $n$ ) are estimated from next relation using the real ( $\epsilon_1$ ) and imaginary ( $\epsilon_2$ ) parts of the dielectric function:

$$\alpha(\omega) = \sqrt{2}\omega \left[ \sqrt{\epsilon_1^2 + \epsilon_2^2} - \epsilon_1 \right]^{0.5} \quad (1)$$

$$n(\omega) = \left[ \frac{\epsilon_1(\omega)}{2} + \frac{\sqrt{\epsilon_1^2(\omega) + \epsilon_2^2(\omega)}}{2} \right]^{0.5} \quad (2)$$

$$\epsilon_1(\omega) = 1 + \frac{2}{\pi} \int_0^\infty \frac{\omega'}{\omega'^2 - \omega^2} d\omega' \quad (3)$$

$$\epsilon_2(\omega) = \frac{2e^2\pi}{\Omega\epsilon_0} |\langle \Psi_k^c | \mathbf{u} \times \mathbf{r} | \Psi_k^v \rangle| \delta(E_k^c - E_k^v - E) \quad (4)$$

where  $\omega$  is the angular frequency,  $\mathbf{u}$  is vector represented the polarization of the incident electric field,  $\mathbf{r}$  is the position operator,  $\Psi_k^c$  and  $\Psi_k^v$  are the probable transitions between valence and conduction bands.  $\epsilon_0$ ,  $e$  and  $\Omega$  are the dielectric constant in free space, charge of electron and volume of the unit cell.

The correlation between extinction coefficient ( $k$ ) and the absorption of light can be estimated as the following:

$$k = \frac{\alpha \lambda}{4\pi} \quad (5)$$

The optical conductivity can be estimated using the dielectric constant  $\varepsilon(\omega)$  as the following:

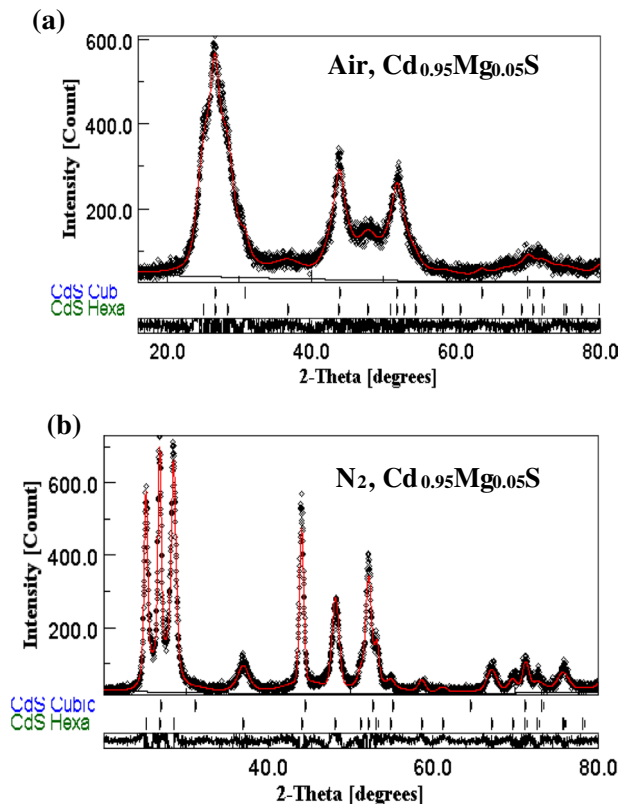
$$\sigma(\omega) = -i \frac{\omega}{4\pi} |\varepsilon(\omega) - 1| \quad (6)$$

### 3 Results and discussion

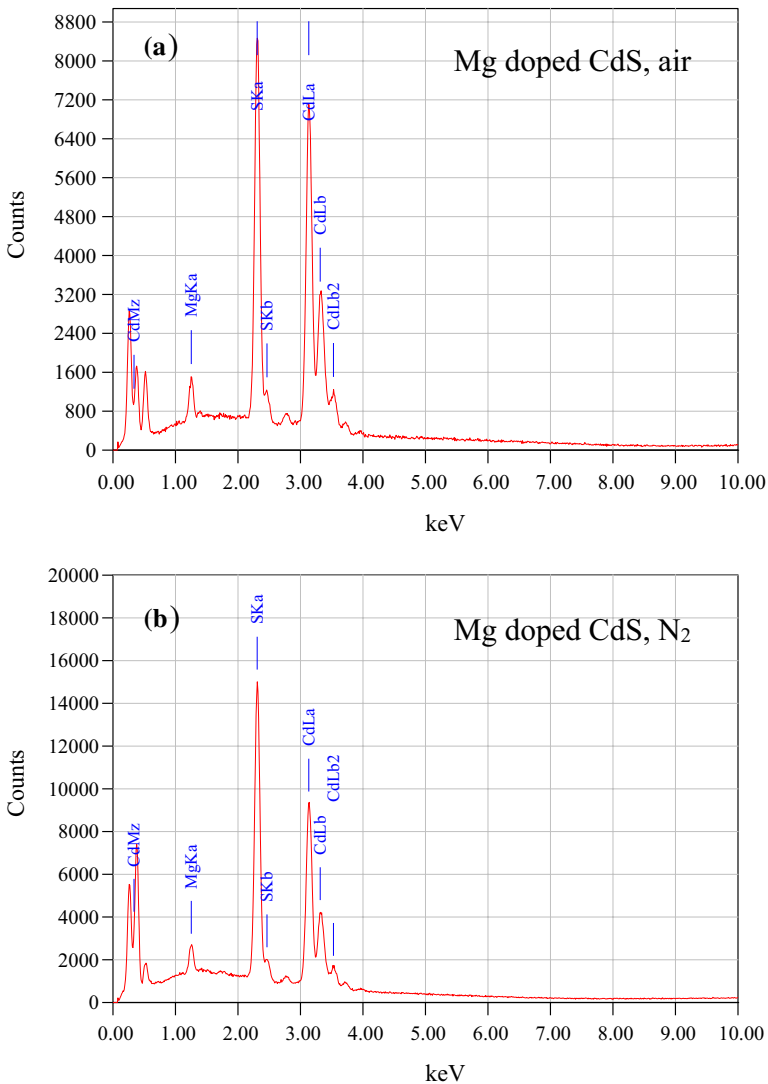
#### 3.1 X-ray diffraction and morphological investigations

Figure 1 illustrates the x-ray diffraction patterns fitting obtained from Rietveld refinement for the nano powder  $\text{Cd}_{0.95}\text{Mg}_{0.05}\text{S}$  prepared in the open air and under nitrogen. Although the patterns look like a single hexagonal phase, two phases were identified as cubic zinc blende and hexagonal wurtzite phases. Moreover, one can notice from the diffraction patterns that the samples prepared under nitrogen gas are much better in crystallinity than that prepared in air. No other phases were detected implying the incorporation of Mg ions

**Fig. 1** Rietveld refinement for CdS and Mg-doped CdS formed in **a** air and **b**  $\text{N}_2$  flow



substitutionally for Cd in the CdS lattice, a result was confirmed by Rietveld analysis. Moreover, Fig. 2 depicts the elemental analysis obtained for the samples which emphasize the incorporation of Mg into the CdS lattice with elements percentages intended in preparation. Table 1 reveals the refined structural parameters got using Rietveld refinement procedure. The cell parameters and z-coordinate of S ions were reduced for both phases as it doped with Mg ion owing to its smaller radius with respect to Cd ion. Furthermore, the cell parameters for the samples prepared under nitrogen flow are smaller than those for samples obtained in air, which may be ascribed to lesser defects present in samples in the case of  $N_2$  gas atmosphere. This claim is confirmed by the much bigger crystallite size for samples



**Fig. 2** EDS spectra for Mg-doped CdS formed in **a** air and **b**  $N_2$  flow

**Table 1** Lattice parameters (a, c), crystallite size, z coordinate, and percentage of different phases (%) for CdS and Cd<sub>0.95</sub>Mg<sub>0.05</sub>S samples prepared in air and N<sub>2</sub> circumstances

	Cd <sub>0.95</sub> Mg <sub>0.05</sub> S							
	Cubic $F\bar{4}3m$			Hexa P 6 <sub>3</sub> m c				
	a (Å)	size (nm)	%	a (Å)	c (Å)	size (nm)	z	%
Air								
Undoped CdS	5.8847(4)	7.1	43	4.1728(3)	6.7891(4)	7.8	0.3876	57
Mg-doped CdS	5.8677	6.1	57	4.1631	6.7811	4.1	0.3563	43
N <sub>2</sub> circumstance								
Undoped CdS	5.8750	35.1	3.5	4.1628	6.7576	17.3	0.3946	96.5
Mg-doped CdS	5.8494	36.8	29	4.1430	6.7300	14.7	0.3414	71

formed under nitrogen as shown in Table 1. Inspecting Table 1, one can notice that the phase percentages of cubic and hexagonal phases are almost equal in the case of samples formed in air, while for samples synthesized under N<sub>2</sub> the hexagonal phase is dominant. For pure CdS prepared in N<sub>2</sub>, the sample has almost hexagonal structure with a tiny part of the cubic phase.

### 3.2 UV absorption study

The direct optical band gap ( $E_g$ ) for Mg-doped CdS synthesis in air or under nitrogen atmosphere was evaluated from UV–Vis absorption measurements utilizing the Tauc's formula (Tauc. 1972):

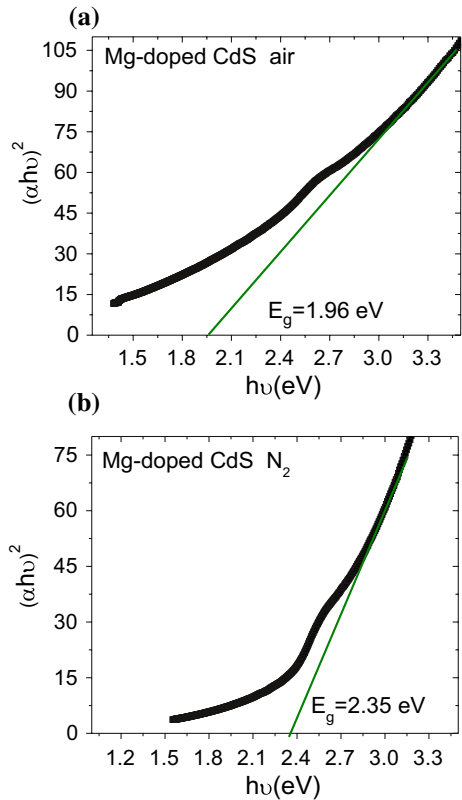
$$\alpha h\nu = A(h\nu - E_g)^{0.5} \quad (7)$$

$$\alpha = 2.303xA/t$$

where  $\alpha$ ,  $h\nu$  and  $A$  are the absorption coefficient, the incident photon energy and a constant, respectively.

By plotting a relation between  $(\alpha h\nu)^2$  and  $h\nu$ , the direct optical band gap can be calculated by extending the linear part of  $(\alpha h\nu)^2$  to 0 with x-axis as demonstrated in Fig. 3. The obtained energy gaps are 1.95 and 2.35 eV for 5%Mg doping samples formed in air and N<sub>2</sub>, respectively, relative to undoped samples, 2.58 eV (CdS, air) and 2.12 eV (CdS, N<sub>2</sub>) (Mohamed et al. 2018), respectively. As revealed from the result, the optical band gap was decreased as the undoped sample prepared in N<sub>2</sub> relative to the undoped one prepared in air. The reason for the reduction in the optical band gap of CdS (N<sub>2</sub>) sample as compared with CdS (air) sample is owing to the increasing of particle size of the sample formed using N<sub>2</sub> flow relative to the sample formed in air (Wang et al. 2008) as listed in Table 1. On the other hand, the optical band gap decreased as CdS (air) doped with Mg, while the optical band gap of CdS (N<sub>2</sub>) was increased as it doped with Mg. Previously, it was found that the optical band gaps of CdS doped with 10%Mg (air or N<sub>2</sub> atmosphere) were enhanced as it doped with 10%Mg (Mohamed et al. 2018). The optical band gaps of CdS, Ga<sub>2</sub>O<sub>3</sub> thin film, ZnO and TiO<sub>2</sub> were enhanced as they doped with Mg (Sivaraman et al. 2016; Bi et al. 2018; Manju et al. 2018; Zeng et al. 2016). On the other hand, the energy gaps of CdSe and

**Fig. 3** Relation between  $(\alpha h\nu)^2$  and  $h\nu$  of Mg-doped CdS formed in **a** air and **b**  $N_2$  flow



$TiO_2$  film were reduced as they doped with Mg (Murugan et al. 2001; Joo et al. 2003). Furthermore, the optical band gap of ZnS was reduced from 3.94 to 3.72 eV then it increased again to 3.86 eV as the concentration of Mg doping raised in the matrix (Ashokkumar and Boopathyraja 2018). The increase in energy gap may be explained by Burstein–Moss (BM) effect (Sivaraman et al. 2016). Magnesium ion has less electro-negativity as compared with Cd ion. Consequently, the Mg ions shared further electrons than the Cd ions in the conduction band which caused a shift in the Fermi level thus raised the optical band gap energy of the doped sample (Sivaraman et al. 2016). Furthermore, the red and blue shifts in the energy gap may be owing to the size effect dependent, the percentage of cubic phase to the hexagonal phase of CdS in the sample and the existence of some oxygen in the sample due to the preparation of some samples in the air (Ashokkumar and Boopathyraja 2018). Further investigation of the reason of the increasing or decreasing in the value of the optical band gap as Mg-doped CdS in air or under  $N_2$  flow will be explored in the electronic section.

### 3.3 Photoluminescence investigation

Figure 4 exhibits the photoluminescence (PL) spectra for CdS and Mg-doped CdS samples (air or  $N_2$ ) using 350 nm as an excitation wavelength. It can observe that the intensity of the PL emission of CdS sample prepared under  $N_2$  flows is higher than the intensity of CdS

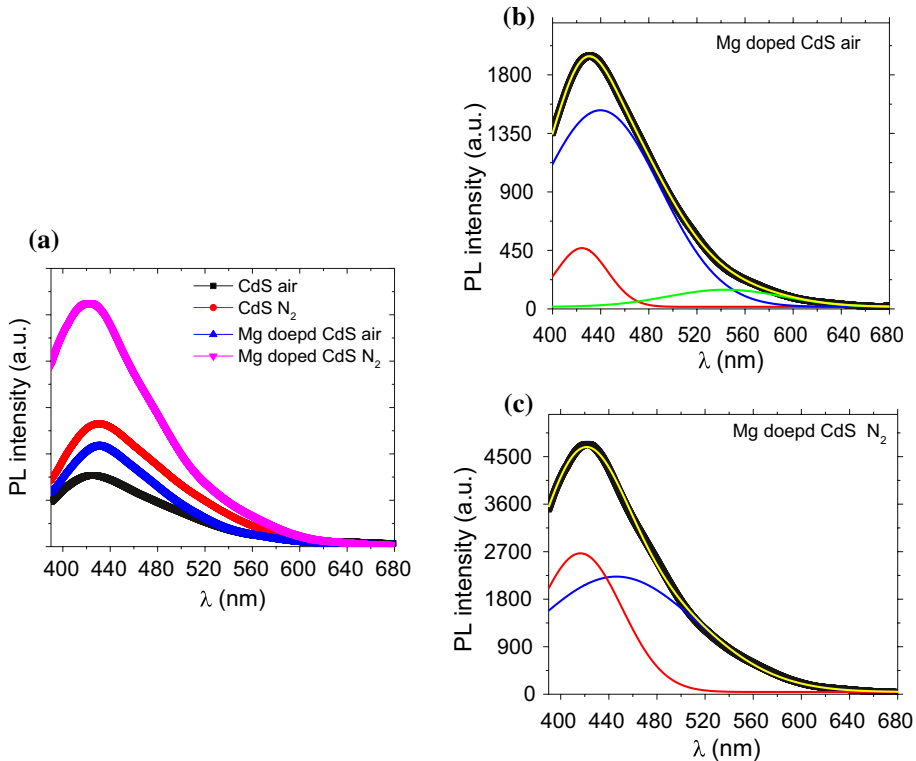


**Fig. 4** a The photoluminescence measurements and b, c Gaussian fitting for Mg-doped CdS formed in air and  $N_2$  flow

formed in air. Moreover, the PL intensity increased further in Mg doped sample prepared under nitrogen flow. It is recognized that the PL intensity and the ratio of the electron-hole recombination rate have a direct relation; as the recombination rate increased, the PL intensity enhanced. Furthermore, the PL intensity affected by the preparation's technique and the kind of the doping elements. For example, Mg-doped ZnS formed applying hydrothermal procedure exhibited an improvement in the PL intensity owing to the creation of novel radiation centers (Heiba et al. 2015b). Furthermore, as Mg-doped nano CdSe, the PL intensity was enhanced as compared with the undoped one (Kwak et al. 2007). The emissions of undoped and doped samples (air and  $N_2$ ) can be analyzed applying Gaussian function into (violet, two blues), (violet, blue), (two violets, green) and (two violets) sub emissions, respectively. Previously, it was found that the CdS doped sample with 10%Mg, emitted violet and blue colors whether it produced in the air or underflow of  $N_2$  (Mohamed et al. 2018). CdS quantum dots formed using other techniques emitted almost similar or different emissions (López and Gómez 2014; Zhang et al. 2008; Mishra et al. 2011). For example; CdS quantum dots prepared using a post-synthesis modification technique with assist of NaOH solution exhibited violet-blue and orange-red emissions (López and Gómez 2014). When a ligand exchange method is applied to CdS, a strong violet color was observed (Zhang et al. 2008). CdS quantum dots produced by a Co-precipitation procedure emitted blue, green and yellow emissions (Mishra et al. 2011; Katari et al. 1994). Conversely,



Mg-doped CdS–PVA emitted a green color (Krishnakumar et al. 2017). In addition, Mg-doped CdS formed using the co-precipitation technique exhibited green to red color owing to the imperfections in the samples (Mishra et al. 2011). The violet color can be ascribed to the band edge transition that resulted from the recombination of excitons or shallowly trapped electron–hole pairs (Krishnakumar et al. 2017). Alternatively, the blue emission caused by donor, acceptor and trap states (Lie et al. 2005).

### 3.4 Electronic analysis

In this study, the zinc-blende structure with F-43 m space group is used as a starting model for the undoped and Mg-doped CdS samples. In order to understand the behavior of the energy gap of doped samples as revealed in Fig. 3 (UV part), four cases were studied: Some Mg ions substituted some Cd ions in (i) stoichiometric CdS matrix, (ii) nonstoichiometric  $\text{Cd}_{1-\delta}\text{S}$  (some cadmium deficiency), (iii) nonstoichiometric  $\text{CdS}_{1-\delta}$  (some sulfur deficiency) and (iv) non-stoichiometric  $\text{CdS}_{1-\delta}\text{O}_\delta$  (some sulfur deficiency and some oxygen enter the empty space). The initial structure data was obtained from XRD study, Table 1. After geometry relaxation for undoped and doped samples in all previously mentioned cases. The calculated lattice parameter are 5.91, 5.83, 5.64, 5.73, 5.80 Å for CdS and Mg-doped ( $\text{CdS}$ ,  $\text{Cd}_{1-\delta}\text{S}$ ,  $\text{CdS}_{1-\delta}$  and  $\text{CdS}_{1-\delta}\text{O}_\delta$ ) samples, respectively. The obtained lattice parameters from the current DFT calculation for CdS is smaller than the lattice parameters for the same material obtained previously from other theoretical studies for instance 6.0 Å or 5.976 Å (Jiang et al. 2016; Han et al. 2014) and it was somewhat different from the experimental result got from the current XRD study. The lattice parameter of Mg/CdS samples in this study is less than that of undoped sample, because of the difference between the ionic radii of Mg and Cd ions as was investigated in detail in XRD part. The spin-polarized band structures for undoped and doped samples in the current study have been evaluated in first Brillouin zone through the high symmetry direction. The red dashed line in the band structure in Fig. 5 is standing for the Fermi energy level. Figure 5a revealed the band structure of CdS sample, where the sample exhibited a semiconductor characteristic with a direct band gap; the valence band maximum (VBM) and the conduction band minimum (CBM) situated at a similar high symmetry  $\Gamma$  point. Moreover, the band gap value of CdS is 1.142 eV which in agreement with other previous theoretical studies (1.11 or 1.12 or 1.45 eV (Heyd et al. 2005; Noor et al. 2012; Deligoz et al. 2006)), but it difference from the results obtained from experimental part (2.58 and 2.12 eV for undoped sample annealed in air and  $\text{N}_2$ , respectively, Fig. 3). The low value of the theoretical energy gap is predicted as the band gap is underestimation in DFT calculations as a result of the recognized limitation of expecting the precise energy band features (Heiba et al. 2020a). Figure 5 also shows that the Mg-doped CdS samples in all mentioned cases have direct band gap structure. Furthermore, all samples have a semiconductor nature except Mg-doped  $\text{Cd}_{1-\delta}\text{S}$ , it has a metallic nature (Heiba et al. 2020b). The obtained theoretical energy gaps are 1.457, 1.913 and 1.051 eV for Mg-doped CdS,  $\text{CdS}_{1-\delta}$  and  $\text{CdS}_{1-\delta}\text{O}_\delta$  samples, respectively. Where, the energy gap increased in all cases except the sample contained oxygen, the band gap energy decreased.

Figure 6 reveals the density of states (DOS) with spin-up and down for CdS and Mg-doped CdS (in the current study). As shown from the figure that all samples in all cases are completely symmetrical, consequently all samples are non-magnetic. Figure 7 reveals the energy dependent of optical absorption for CdS and Mg-doped CdS (stoichiometric

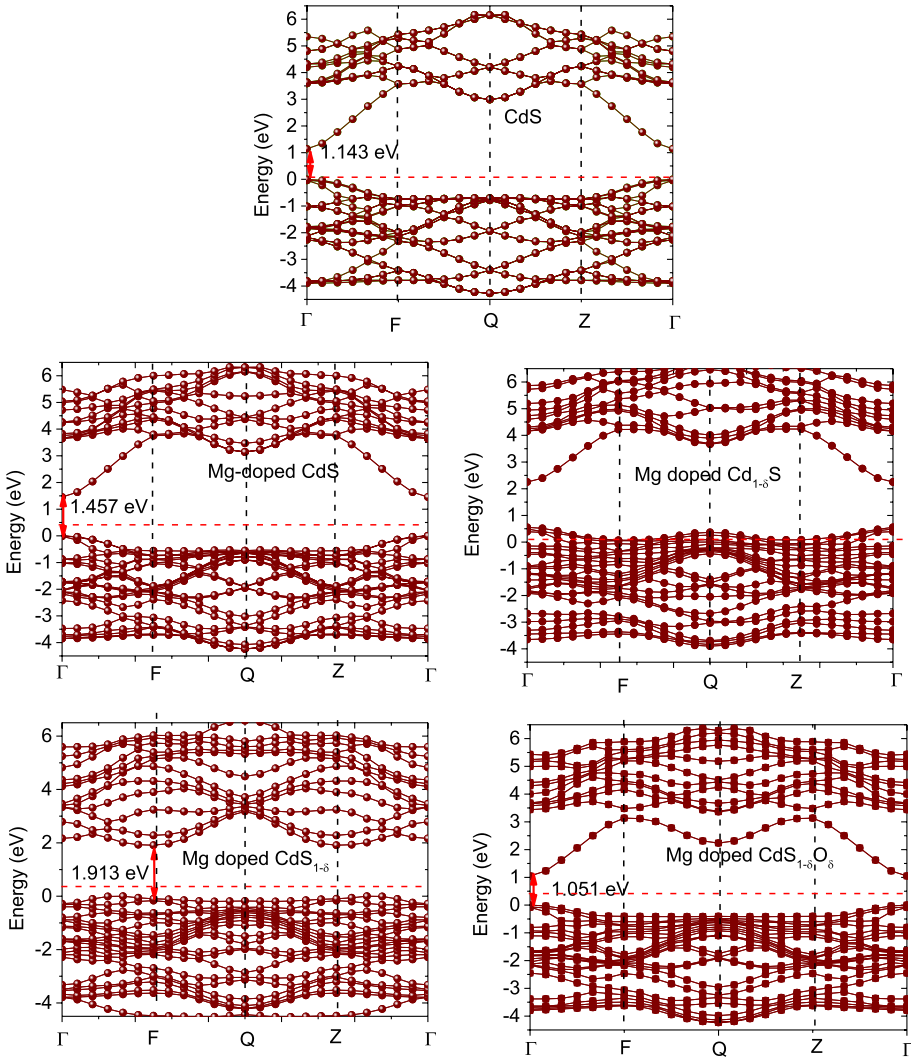


**Fig. 5** The electronic band structure of CdS and Mg-doped CdS (stoichiometric and non-stoichiometric)

or non-stoichiometric). The obtained absorption spectra may result from the excitation of electrons from the valence to conduction band (Khan et al. 2016).

The absorption spectra for all studied cases exhibited an increasing trend up to specific energy value then it reduced. It is observed also that the absorption spectra of all Mg-doped samples are shifted toward the higher energy (blue shift) as compared with CdS sample except Mg-doped CdS<sub>1- $\delta$</sub>  sample. Where Mg-doped CdS<sub>1- $\delta$</sub>  sample revealed a red-shift in the intermediate energy range and blue shift in the high energy range. The blue shift is pointed to the increase of the particle size and it is a signature of the formation of the nano structure sample, while the red shift may be caused by a reduction in the difference of energy levels upon applied electric field (Khan et al. 2019). Beyond the maximum of the absorption spectra, the absorption decreased for higher energy values. The extra

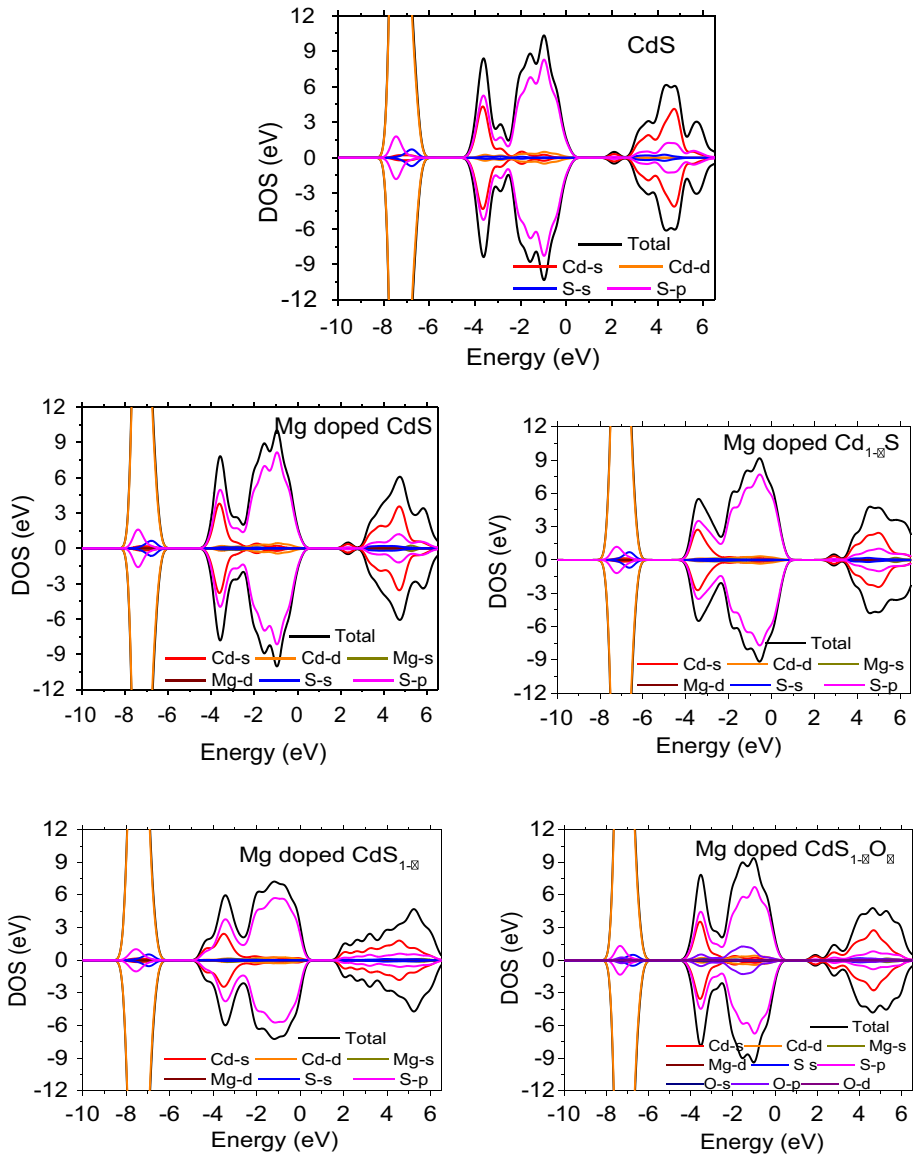
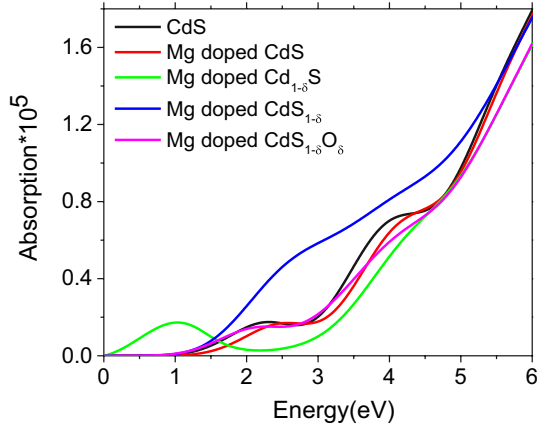


**Fig. 6** Total (DOS) and partial density of states (PDOS) of CdS and Mg-doped CdS (stoichiometric and non-stoichiometric)

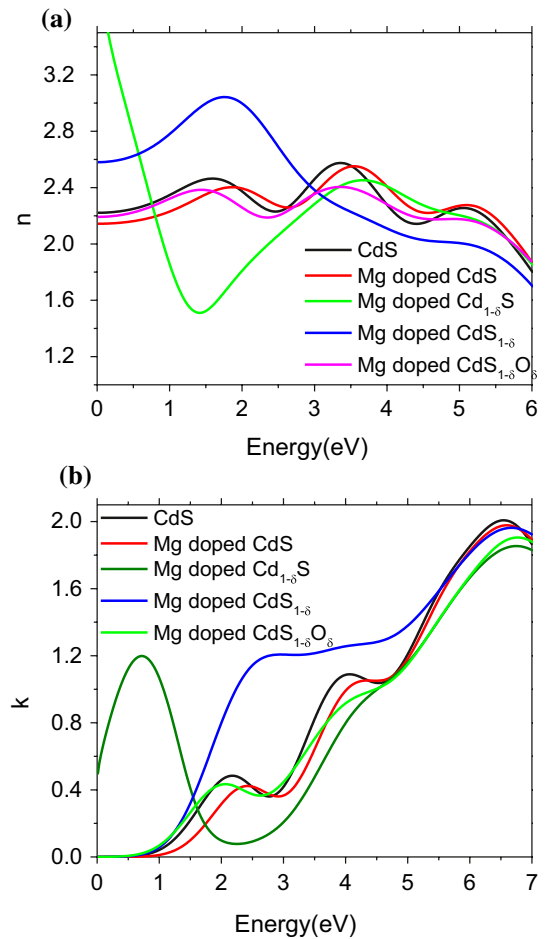
peak appeared in the low energy range for Mg-doped  $\text{CdS}_{1-x}$  is due to the presence of Mg ions and vacancies together in CdS matrix, an analogous result was got in Mn-doped non-stoichiometric ZnS (Heiba et al. 2020b). Also the extra peak appeared in the visible range for Mg-doped  $\text{CdS}_{1-x}$  is due to the dramatic changes in the DOS of the sample as revealed in Fig. 5.

Figure 8a shows the change of refractive index ( $n$ ) with energy for all samples. The index of refraction was rose upon increasing the photon energy (eV) until it reached its

**Fig. 7** The absorption spectra for CdS and Mg-doped CdS (stoichiometric and non-stoichiometric)



**Fig. 8 a** The refractive index (n) and **b** extinction coefficient (k) for CdS and Mg-doped CdS (stoichiometric and non-stoichiometric)



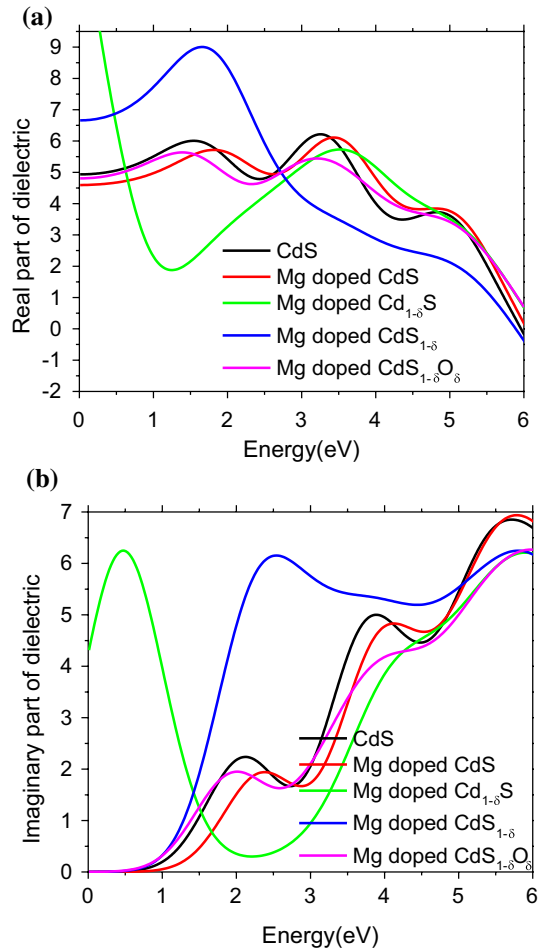
highest value, then it decreased in all samples except Mg-doped  $\text{Cd}_{1-\delta}\text{S}$ , it reduced then enhanced until a specific limit then it decreased once more similar to the other samples. The change in the refractive index value may appear owing to the dispersion of the light deeper within the material. Therefore numerous interactions occurred inside the unit cell. The highest refractive indices value for CdS and Mg-doped  $\text{CdS}_{1-\delta}$  samples are 2.6 at 368 nm and 3.03 at 705 nm. It was found previously, the theoretical index of refraction for undoped sample is larger than the experiment result obtained from CdS thin film (Khan et al. 2019).

As revealed from the Eq. (5), there is a correlation between  $\alpha$  and  $k$  parameters, therefore a great similarity between the behaviors of  $\alpha$  and  $k$  can be noticed. The photon energy dependence of the extinction coefficient was represented in Fig. 8b. The extinction coefficient results of the current samples gradually increased as the photon energy rose until it attained its highest value then it decreased with more increase in the photon energy. A tiny peak in the low energy range was appeared in Mg-doped  $\text{Cd}_{1-\delta}\text{S}$  sample and another peak was observed in the visible range in the case of Mg-doped  $\text{CdS}_{1-\delta}$  sample. The appearance of these extra peaks may be owing to the localization of the density of states close to the Fermi level in Mg/ $\text{Cd}_{1-\delta}\text{S}$  sample and the change of DOS in the case of Mg-doped  $\text{CdS}_{1-\delta}$  sample as shown in Fig. 5. Furthermore, the reduction in the intensity of the highest peak of CdS sample as it doped with Mg may be due to the interactions between different atoms.

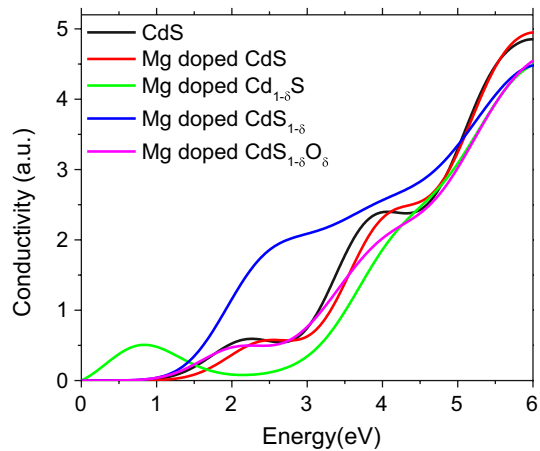
Figure 9a reveals the real dielectric constant ( $\epsilon_1$ ) as function of energy for all samples. The dielectric of CdS and Mg-doped ( $\text{CdS}$  and  $\text{CdS}_{1-\delta}\text{O}_\delta$ ) samples exhibited nearly a similar trend with a small shift but the other two samples (Mg-doped  $\text{Cd}_{1-\delta}\text{S}$  or  $\text{CdS}_{1-\delta}$ ) have different features. The dielectric of all samples may decrease or increase depending on the energy region. In addition, the real dielectric constant exhibited negative results in a definite energy range depend on kind of the sample. The negative results indicate that the reflected incident radiations displayed a metallic character as a result of the incompatibility of the sample's bandgap with the energy of the incident wave (Saikia and Borah 2018). As revealed from the figure, the static dielectric constant has a maximum value in Mg-doped  $\text{Cd}_{1-\delta}\text{S}$  sample and a minimum value in Mg-doped CdS sample. Figure 9b reveals the energy dependent of the imaginary part of the dielectric parameter for all samples. As demonstrated from the figure, undoped samples revealed three peaks. In addition, Mg-doped ( $\text{CdS}$  and  $\text{CdS}_{1-\delta}\text{O}_\delta$ ) samples have an analogous characteristic but the peak positions are changed relative to the undoped sample. These three peaks are emerged into two peaks in the case of Mg-doped  $\text{CdS}_{1-\delta}$  sample at 2.45 and 5.76 eV. Finally, Mg-doped  $\text{Cd}_{1-\delta}\text{S}$  sample has also three peaks but at 5.77, 4.4 and 0.43 eV. Furthermore, the first peak of  $\epsilon_2$  corresponded to the optical band gap, which is the threshold for optical transition between VBM and CBM (Deb and Sarkar 2021; Deb et al. 2020). The optical band gap of CdS, Mg-doped ( $\text{CdS}$ ,  $\text{Cd}_{1-\delta}\text{S}$ ,  $\text{CdS}_{1-\delta}$  and  $\text{CdS}_{1-\delta}\text{O}_\delta$ ) samples are 2.1, 2.38, 2.5, 0.47 and 2.01 eV, respectively. Therefore, the reduction in the optical band gap of the Mg-doped CdS sample annealed in the air (UV part) is may be due to the existence of the oxygen inside the sample or existence of some sulfur deficiency in the sample.

Figure 10 illustrates the optical conductivity ( $\sigma(\omega)$ ) of pure CdS together with Mg-doped samples in the current study. As demonstrated from the figure that the conductivity for all samples was increased with increased photon energy until it attained its highest value then it decreased. The well-defined peak appeared in UV region is due to interband transitions. On the other hand, in the ultraviolet region, the optical conductivity was decreased in all doped samples except Mg-doped CdS sample, it enhanced slightly. In the visible range,

**Fig. 9** **a** The real and **b** imaginary dielectric parts for CdS and Mg-doped CdS (stoichiometric and non-stoichiometric)



**Fig. 10** The conductivity for undoped and Mg-doped CdS (stoichiometric and non-stoichiometric)



the photoconductivity was decreased except Mg-doped CdS<sub>1-δ</sub> sample is largely enhanced. Finally, Mg-doped Cd<sub>1-δ</sub>S sample exhibited a photoconductivity response in the IR range.

## 4 Conclusion

Rietveld refinement revealed that all XRD patterns of Cd<sub>0.95</sub>Mg<sub>0.05</sub>S sample formed in air and under nitrogen have two phases (cubic zinc blende and hexagonal wurtzite). The phase fractions of cubic and hexagonal phases are almost equal in the case of samples formed in the air, while for samples formed in the existence of nitrogen the hexagonal phase is dominant. The samples prepared under nitrogen gas are much better in crystallinity than prepared under air. The cell parameters and the z-coordinate of S ions were reduced upon doping the samples with Mg. FTIR confirmed the existence of Cd-S vibration band in all samples. Analysis of UV-Vis absorption spectra disclosed the optical band gap of CdS sample prepared in N<sub>2</sub> is less relative to sample prepared in air. Also, upon doping with Mg, the optical band gap of CdS (air) sample decreased while it increased for CdS (N<sub>2</sub>) sample. The optical band gaps for 5%Mg-doped CdS (air) and 5%M-doped CdS (N<sub>2</sub>) samples are 1.95 and 2.35 eV, respectively. The red or blue shifts in the energy gaps may be owing to the size effect dependence, the percentage of cubic to hexagonal phase in CdS sample and the existence of some oxygen in the sample prepared air. The PL intensity of CdS sample was enhanced when it doped with Mg. The PL intensity of Mg-doped sample formed under nitrogen has a maximum value as compared with other samples. Undoped and Mg-doped CdS samples formed in air or N<sub>2</sub> flow exhibited (violet, two blues), (violet, blue), (two violets, green) and (two violets) sub emissions, respectively. DFT showed that the energy gap increased in Mg-doped (CdS, Cd<sub>1-δ</sub>S and CdS<sub>1-δ</sub>) while it decreased in Mg-doped CdS<sub>1-δ</sub>O<sub>δ</sub> sample. Mg-doped CdS samples in all cases (CdS, CdS<sub>1-δ</sub> and CdS<sub>1-δ</sub>O<sub>δ</sub>) have the direct band gap structure and non-magnetic nature. Mg-doped (CdS, CdS<sub>1-δ</sub> and CdS<sub>1-δ</sub>O<sub>δ</sub>) samples have a semiconductor nature while Mg-doped Cd<sub>1-δ</sub>S has a metallic nature. Mg-doped CdS<sub>1-δ</sub> has the highest refractive index. The photoconductivity of Mg-doped CdS<sub>1-δ</sub> is largely enhanced in the visible range while Mg-doped Cd<sub>1-δ</sub>S sample exhibited a photoconductivity response in the IR range.

**Acknowledgements** The authors acknowledge Taif University Research Supporting Project number (TURSP-2020/66), Taif University, Taif, Saudi Arabia.

## References

- Ashokkumar, M., Boopathyraja, A.: Structural and optical properties of Mg doped ZnS quantum dots and biological applications. *Superlattices Microstruct.* **113**, 236–243 (2018)
- Banerjee, R., Jayakrishnan, R., Ayyub, P.: Effect of the size-induced structural transformation on the band gap in CdS nanoparticles. *J. Phys. Condens. Matter* **12**(50), 10647–10654 (2000)
- Bi, X., Wu, Z., Huang, Y., Tang, W.: Stabilization and enhanced energy gap by Mg doping in ε-phase Ga<sub>2</sub>O<sub>3</sub> thin films. *AIP Adv.* **8**(2), 025008(1–5) (2018)
- Deb, J., Sarkar, U.: Boron-nitride and boron-phosphide doped twin-graphene: applications in electronics and optoelectronics. *Appl. Surf. Sci.* **541**, 148657(1–12) (2021)
- Deb, J., Paul, D., Sarkar, U.: In: *AIP Conference Proceedings* 1953, p. 030235(1–5) (2018)
- Deb, J., Paul, D., Sarkar, U.: Pentagraphyne: a new carbon allotrope with superior electronic and optical property. *J. Mater. Chem. C* **8**, 16143–16150 (2020)
- Deligoz, E., Colakoglu, K., Ciftci, Y.: Elastic, electronic, and lattice dynamical properties of CdS, CdSe, and CdTe. *Phys. B* **373**, 124–130 (2006)

- Devadoss, I., Sakhivel, P.: Effect of Mg on Cd<sub>0.9-x</sub>Zn<sub>0.1</sub>S nanoparticles for optoelectronic applications. *Appl. Phys. A* **126**, 315(1–8) (2020)
- Garg, P., Kumar, S., Choudhuri, I., Mahata, A., Pathak, B.: Hexagonal planar CdS monolayer sheet for visible light photocatalysis. *J. Phys. Chem. C* **120**(13), 7052–7060 (2016)
- Giribabu, G., Amaranatha Reddy, D., Murali, G., Vijayalakshmi, R. P.: Structural and optical studies on Mg doped CdS nanoparticles by simple co-precipitation method. In: *AIP Conference Proceedings*, vol. 1512, pp. 186–187 (2013)
- Han, Y.X., Yang, C.L., Sun, Y.T., Wang, M.S., Ma, X.G.: The novel optical properties of CdS caused by concentration of impurity Co. *J. Alloys Compd.* **585**, 503–509 (2014)
- Heiba, Z.K., Mohamed, M.B., Imam, N.G.: Biphasic quantum dots of cubic and hexagonal Mn doped CdS; necessity of Rietveld analysis. *J. Alloys Compd.* **618**, 280–286 (2015a)
- Heiba, Z.K., Mohamed, M.B., Imam, N.G.: Defect based violet–blue emission of Mg doped ZnO annealed at different temperatures. *J. Mater. Sci. Mater. Electron.* **26**(9), 6344–6351 (2015b)
- Heiba, Z.K., Mohamed, M.B., Wahba, A.M.: Structural, optical, mechanical, and electronic properties of Cr-doped alumina. *J. Mater. Sci. Mater. Electron.* **31**(17), 14645–14657 (2020a)
- Heiba, Z.K., Mohamed, M.B., Ahmed, S.I., Albassam, A.A.: Structural, optical, and electronic properties of non-stoichiometric nano-ZnS<sub>1-x</sub>Mn<sub>x</sub>. *J. Mater. Sci. Mater. Electron.* **31**(16), 13447–13459 (2020b)
- Heyd, J., Peralta, J.E., Scuseria, G.E.: Energy band gaps and lattice parameters evaluated with the Heyd-Scuseria-Ernzerhof screened hybrid functional. *J. Chem. Phys.* **123** (2005) 174101(1–8).
- Jiang, X.-Y., Yang, C.-L., Han, Y.-X., Wang, M.-S., Ma, X.-G.: Enhancement of absorption and conductivity of CdS in the infrared range with Cu dopant. *Mater. Chem. Phys.* **183**, 349–355 (2016)
- Joo, J., Na, H.B., Yu, T., Yu, J.H., Kim, Y.W., Wu, F., Zhang, J.Z., Hyeon, T.: Generalized and facile synthesis of semiconducting metal sulfide nanocrystals. *J. Am. Chem. Soc.* **125**, 11100–11105 (2003)
- Katari, J.E.B., Colvin, V., Alivisatos, A.P.: X-ray photoelectron spectroscopy of CdSe nanocrystals with applications to studies of the nanocrystal surface. *Chem. Phys.* **98**, 4109–4117 (1994)
- Khan, M.J.I., Babar, S., Nabi, A., Rana, A.M., Iqbal, M., Rehman, S.U., Ahmad, J.: Theoretical studies of optical properties of Cu doped rocksalt CdS. *J. Alloys Compd.* **695**, 3605–3611 (2016)
- Khan, M.J.I., Kanwal, Z., Usmani, M.N., Zeeshan, M., Yousaf, M.: An insight into optical properties of Pb:CdS system (a theoretical study). *Mater. Res. Express* **6**(6), 065904 (2019)
- Kobyakov, P.S.: Deposition and characterization of Cd<sub>1-x</sub>Mg<sub>x</sub>Te thin films grown by a novel cosublimation method. *J. Vacuum Sci. Technol. A* **32**, 02151(1–17) (2014)
- Krishnakumar, V., Ranjith, R., Jayaprakash, J., Boobas, S., Venkatesan, J.: Enhancement of photocatalytic degradation of methylene blue under visible light using transparent Mg-doped CdS–PVA nanocomposite films. *J. Mater. Sci. Mater. Electron.* **28**, 13990–13999 (2017)
- Kwak, W.-C., Kim, T.G., Chae, W.-S., Sun, Y.-M.: Tuning the energy bandgap of CdSe nanocrystals via Mg doping. *Nanotechnology* **18**, 205702(1–4) (2007)
- Li, W., Li, D., Chen, Z., Huang, H., Sun, M., He, Y., Fu, X.: High-efficient degradation of dyes by Zn<sub>x</sub>Cd<sub>1-x</sub>S solid solutions under visible light irradiation. *J. Phys. Chem. C* **112**, 14943–14947 (2008)
- Li, Q., Guo, B.D., Yu, J.G., Ran, J.G., Zhang, B.H., Yan, H.J., Gong, J.R.: Highly efficient visible-light-driven photocatalytic hydrogen production of CdS-cluster-decorated graphene nanosheets. *J. Am. Chem. Soc.* **133**, 10878–10884 (2011)
- Lie, Y., Chim, W. K., Sun, H. P., Wilde, G.: Highly ordered CdS nanoparticle arrays on silicon substrates and photoluminescence properties. *Appl. Phys. Lett.* **86** (2005)103106 (1–3).
- López, I., Gómez, I.: Improvement of the luminescent properties of cadmium sulfide quantum dots by a post-synthesis modification. *Phys. B* **453**, 81–85 (2014)
- Lutterotti, L.: Total pattern fitting for the combined size–strain–stress–texture determination in thin film diffraction. *Nucl. Inst. Methods Phys. Res. B.* **268**, 334–340 (2010)
- Manju, J., Mi, S., Jawhar, J.: Synthesis of magnesium-doped TiO<sub>2</sub> photoelectrodes for dye-sensitized solar cell applications by solvothermal microwave irradiation method. *J. Mater. Res.* **33**(11), 1534–1542 (2018)
- Mishra, S.K., Srivastava, R.K., Prakash, S.G., Yadav, R.S., Panday, A.C.: Structural, photoconductivity and photoluminescence characterization of cadmium sulfide quantum dots prepared by a co-precipitation method. *Electron Mater. Lett.* **7**(1), 31–38 (2011)
- Mohamed, M.B., Abdel-Kader, M.H., Alhazime, A.A., Almarashi, J.Q.M.: Effect of preparation methods and doping on the structural and tunable emissions of CdS. *J. Mol. Struct.* **1155**, 666–674 (2018)
- Morales, R.L., Angel, O.Z., Delgado, G.T.: Photoluminescence in cubic and hexagonal CdS films. *Appl. Surf. Sci.* **175–176**, 562–566 (2001)



- Mueller, A.H., Petruska, M.A., Achermann, M., Werder, D., Akhadow, E., Koleske, D., Hoffbauer, M., Klimov, V.I.: Multicolor light-emitting diodes based on semiconductor nanocrystals encapsulated in GaN charge injection layers. *Nano Lett.* **5**(6), 1039–1044 (2005)
- Murphy, C.J.: Optical sensing with quantum dots. *Anal. Chem.* **74**(19), 520A–526A (2002)
- Murugan, A.V., Sonawane, R.S., Kale, B.B., Apte, S.K., Kulkarni, A.V.: Microwave–solvochemical synthesis of nanocrystalline cadmium sulfide. *Mater. Chem. Phys.* **71**(1), 98–102 (2001)
- Noor, N.A., Tahir, W., Aslam, F., Shaukat, A.: Ab initio study of structural, electronic and optical properties of Be-doped CdS, CdSe and CdTe Compounds. *Phys. B* **407**, 943–952 (2012)
- Pan, J., Utama, M.I.B., Zhang, Q., Liu, X., Peng, B., Wong, L.M., Sum, T.C., Wang, S., Xiong, Q.: Composition-tunable vertically aligned CdS<sub>x</sub>Se<sub>1-x</sub> nanowire arrays via van der Waals epitaxy: investigation of optical properties and photocatalytic behavior. *Adv. Mater.* **24**, 4151–4156 (2012)
- Pegu, D., Deb, J., Paul, D., Sarkar, U.: Electronic, nonlinear optical and thermodynamic properties of (CdS)<sub>n</sub> clusters: A first principle study. *Comput. Condens. Matter* **14**, 40 (2018)
- Perdew, J.P., Wang, Y.: Accurate and simple analytic representation of the electron-gas correlation energy. *Phys. Rev. B* **45**, 13244–13249 (1992)
- Perdew, J.P., Burke, K., Ernzerhof, M.: Generalized gradient approximation made simple. *Phys. Rev. Lett.* **77**, 3865–3868 (1996a)
- Perdew, J.P., Burke, K., Wang, Y.: Generalized gradient approximation for the exchange–correlation hole of a many-electron system. *Phys. Rev. B* **54**(23), 16533–16539 (1996b)
- Rodríguez-Carvajal, J.: Recent advances in magnetic structure determination by neutron powder diffraction. *Phys. B* **92**, 55–69 (1993)
- Saikia, D., Borah, J.P.: Carrier-induced ferromagnetism in half-metallic Co-doped ZnS-diluted magnetic semiconductor: a DFT study. *Appl. Phys. A* **124**(3), 240(1–12) (2018)
- Sakthivel, P., Jayasri, T., Madhumitha, J., Mahalakshmi, S., Subhashini, N.: Influence of Cd on optical and photoluminescence behavior of Zn<sub>0.98-x</sub>Cd<sub>x</sub>Mn<sub>0.02</sub>S quantum dots under Ar atmosphere. *Optik* **154**, 74–82 (2018)
- Sivaraman, T., Balu, A.R., Nagarethinam, V.S.: Effect of magnesium incorporation on the structural, morphological, optical and electrical properties of CdS thin films. *Mater. Sci. Semicond. Process.* **27**, 915–923 (2014)
- Sivaraman, T., Nagarethinam, V.S., Balu, A.R.: Properties of CdS films doped with magnesium and fluorine. *Surf. Eng.* **32**(8), 596–600 (2016)
- Tauc, J.: In: A. Abeles (Ed.), *The Optical Properties of Solid*, 1972, p. 277. North Holland, Amsterdam
- Wang, Y., Ouyang, G., Wang, L.L., Tang, L.M., Tang, D.S., Sun, C.Q.: Size- and composition-induced band-gap change of nanostructured compound of II–VI semiconductors. *Chem. Phys. Lett.* **463**, 383–386 (2008)
- Yellaiah, G., Hadasa, K., Nagabhusanam, M.: Growth, characterization, optical and vibrational properties of Sm<sup>3+</sup> doped Cd<sub>0.8</sub>Zn<sub>0.2</sub>S semiconductor compounds. *J. Cryst. Growth* **386**, 62–68 (2014)
- Yücel, Y., Beleli, B.: The role of high Mg level as a dopant on the PbS nanostructures grown by the CBD method. *Mater. Res. Express* **5**(5), 056408 (2018)
- Zeng, W., Yang, X., Shang, M., Xu, X., Yang, W., Hou, H.: Fabrication of Mg-doped ZnO nanofibers with high purities and tailored band gaps. *Ceram. Int.* **42**(8), 10021–10029 (2016)
- Zhang, T.-L., Xia, Y.-S., Diao, X.-L., Zhu, C.-Q.: Preparation and characterization of nano cobalt oxide. *J. Nanopart. Res.* **10**, 59–67 (2008)